Bio-solar green roofs increase solar energy output: the sunny side of integrating sustainable technologies

Fleck. R [1*], Gill. R [1, 2], Pettit. T.J [1] Torpy. F.R [1], Irga. P.J [3]

[1] Plants and Environmental Quality Research Group, School of Life Sciences, University of Technology Sydney

[2] Coastal Oceanography and Algal Research Team, Climate Change Cluster, University of Technology Sydney

[3] Plants and Environmental Quality Research Group, School of Civil and Environmental Engineering, University of Technology Sydney

*Corresponding Author: Robert.Fleck@uts.edu.au

Abstract

In urban spaces, localised energy generation through rooftop solar has become increasingly popular, and green roofs are often used for a range of services such as thermal insulation. In recent years, the adoption of *Bio-solar* green roofs (BSGR) for both thermal insulation and increased solar energy outputs has increased. Here we present two buildings of the same dimensions and location, similar age and construction material, where one hosts a BSGR, and the other a conventional solar roof (CSR) in Sydney, Australia. Each solar array hosted a range of environmental sensors, including ambient temperature and global horizontal irradiance (GHI). The modelled BSGR average hourly energy output was 4.5% higher than the CSR (seasonal trends observed Spring; 4.14%, Summer; 4.16%, and Autumn; 5.21%) with BSGR producing 14.26 MWh more than the CSR, valued at $4,526.22 AUD, and equal to 11.55 t e-CO_2 greenhouse gas mitigation. Further potential for up to 1.55 t of CO_2 could be mitigated by the plant material on the roof, provided the trimming of plant material during maintenance is conducted responsibly. In this instance, the implementation of a BSGR increased the system's solar output by 23.88 kWh per m^2 of panel coverage, as well as reducing the e-CO_2 emissions by 0.019 t per m^2 over the CSR. When compared to the results of previously reported pilot studies and some simulations, it is evident that the implementation of a BSGR is favourable for maximising energy production and the mitigation of GHGs.

Keywords

Bio-solar roof, green roof, photovoltaic, renewable energy, sustainable infrastructure, urban resilience

Abbreviations

BSGR – Bio-solar green roof

CSR – Conventional solar roof

GHI – Global horizontal irradiance

Highlights

- Average BSGR output 4.5% higher than CSR output across all seasons.
- Average BSGR output (kWh) was 4.14, 4.16 and 5.21**%** higher than CSR for Spring, Summer and Autumn.
- BSGR produced 14.26 MWh more than conventional solar, valued at $4,526.22 AUD.
- BSGR reduced 11.55 t e-CO_2 more than CSR. Up to 1.56 t CO_2 was removed by plant biomass.
- BSGR produced 23.88 kWh and reduced 0.019 t e-CO_2 emissions per m^2 of panel coverage more than CSR.

Graphical Abstract

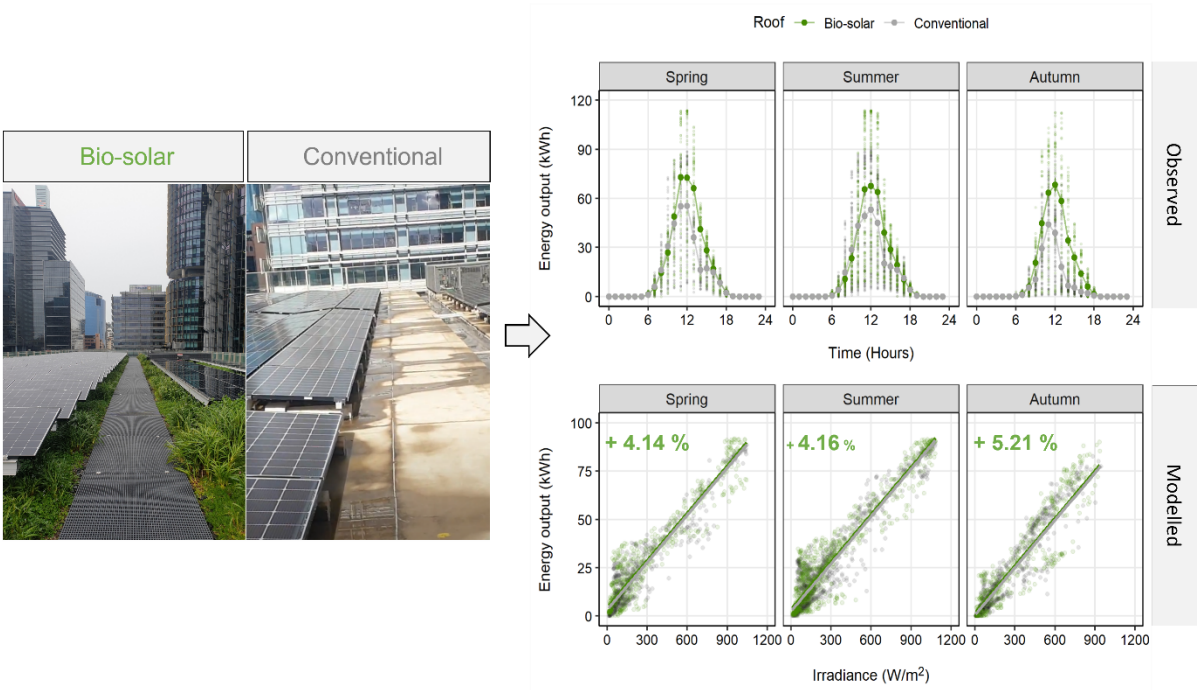

1. Introduction

Non-renewable energy generation, transport and consumption by urban spaces is a significant contributor to greenhouse gas emissions worldwide [1], with urban areas consuming between 67-76% of global energy and generating approximately 75% of the world's carbon emissions [2]. It has been further estimated that 50% of urban energy consumption is attributable to heating, ventilation and air conditioning (HVAC) of buildings [3]. The implementation of a renewable grid will play a major role in reducing future emissions [4], however reducing demand for energy worldwide is often cited as the most effective method to achieve climate targets [5]. In urban spaces, localised energy generation for commercial spaces through rooftop solar has risen in popularity [6], as well as the implementation of various technologies to reduce energy use [7]. For example, green roofs are often used for their range of benefits such as thermal insulation, however in recent years the adoption of *Bio-solar* green roofs (BSGR) for both thermal insulation and increase solar energy outputs has been adopted [8–10].

Green roofs are rooftops that have either been purpose built or retrofitted to facilitate the growth of vegetation. Green roof designs vary, however all consist of a vegetation layer, growth substrate layer, drainage layer, root barrier and waterproof membrane [11]. Green roofs are broadly divided into two categories: intensive (substrate depth ≥ 300 mm), and extensive (substrate depth < 300 mm) [12]. Intensive green roofs often utilise large perennial herbaceous plants, shrubs and small trees [13] and are largely implemented for their aesthetic and biophilic properties [14]. Intensive green roofs require high load-bearing structures and frequent maintenance [15] due to soil depth and plant types, which leads to higher construction and maintenance requirements and initial costs [16]. By contrast, extensive green roofs often utilise grasses and perennial plants. Green roofs are known to provide a myriad of ecosystem services [17], including the removal of air pollutants [13,18,19], urban noise reduction [20–22], increases in urban biodiversity [23,24], serving as a slow-release detention basin for stormwater retention [25–28] and reducing the thermal loading of buildings [29–32].

Extensive green roofs allow for the integration of solar arrays, which together are often termed *Bio-solar* green roofs or Solar-Green Roofs [33]. Bio-solar roofs are theorised to provide greater energy output than conventional solar arrays due to the evapotranspiration of the vegetation which creates a cooler rooftop microclimate [9,34], reducing solar panel temperatures and increasing performance [35]. Bio-solar roofs can also regulate rooftop temperatures through reduced latent heat and lower solar reflectance than conventional concrete roofs [36].

Several experimental and modelling studies have been conducted to assess the performance of bio-solar roofs compared to conventional solar, with varying results. Pilot-scale sized experiments conducted by Alshayeb and Chang [37] found an increase in energy production of 1.4% for model bio-solar roofs; where a study by Chemisana and Lamnatou [38] observed an increase in energy production of 1.29 and 3.33% for 5 day pilot scale experiments on *Gazania* sp. and sedum plots, respectively. While there are several pilot-scale studies that complement these works, there are few that employ the use of commercial or full-scale green

roofs for energy assessments over longer time periods. One study by Hui and Chan [35] simulated a 2,494 m^2 bio-solar roof with varying physical parameters and predicted a maximum performance increase of 4.3% over conventional solar. However, one of the few scale experiments on bio-solar roofs conducted by Perez et al., [39] observed only a 2% increase in performance compared to a conventional system sharing the same roof-space.

Empirical studies have suggested that the differences between bio-solar and conventional solar system performance is variable. There is the possibility that through the use of internal control roof spaces in some studies, the cooling effect of the green roof on the local microclimate could be influencing the control sites, and therefore reducing the observable effect. In addition to this, there are limited studies that have been conducted on roofs of a commercial scale, with the assessment of bio-solar being largely attributed to small subplots with low plant species diversity or leaf area index (LAI), which is known to have an effect on evapotranspiration and the insulative properties of green infrastructure [40,41]. Here we present the unique opportunity to compare two roofs that are spatially unconfounded, with near identical construction and dimensions, with similar age and rooftop infrastructure. In this study we utilise a commercial scale bio-solar roof, as well as an independent control roof in Sydney, Australia to determine the independent effect of a bio-solar installation through both empirical observations and simulations.

2. Methodology

2.1 Site description

This study aimed to compare the solar energy output of sister buildings [42] in Barangaroo, Sydney, Australia. Daramu House was constructed in 2019 and hosted the bio-solar green roof. International House hosted a conventional solar array and was constructed in 2017. These two buildings are the first multi-story commercial timber office buildings in the country and employed near-identical rooftop infrastructure, with differences owing to building maintenance unit (BMU) model and design, exhaust vent placement and machine room design.

This study commenced in Mid-Spring (October), 2020 and concluded in Autumn (May), 2021 for a total of 237 days. For this period, the Barangaroo district received an average of 6.66 sun hours and 4.08 mm of rain per day, with an average evaporation rate of 5.93 mm/day [43]. Average daily temperatures in this region ranged between 9 and 27.43°C [43] during the study period.

Both roofs had a total rooftop surface area of 1,863.35 m^2, with 593.96 m^2 and 567.44 m^2 of solar panel coverage, for the bio-solar and conventional roofs, respectively. Each building employed 0.8 m thick, grey concrete slabs as the bio-solar roof foundation, or roof surface. The bio-solar roof employed an extensive design with a variable substrate depth of 0.1 to 0.12 m and hosted a planted area of 1,460.7 m^2 (78.4% total roof space). On the bio-solar roof, solar panels covered 40.66% of the planted space (Figure 1).

Figure 1. Aerial image of the study site (centre image). Daramu House (bio-solar; left two panels) and International House (conventional solar; right two panels). Sister buildings were near-identical with the exception of roof surface cover (plant material vs concrete). Plant material covers all regions of below panel areas on the bio-solar roof.

The bio-solar roof hosted over 15,000 individual plants and utilised a selection of native grasses and herbaceous plants to attract a diverse faunal community [44], with an estimated LAI of 4.35 [9]. The bio-solar roof also utilised a sub-surface irrigation system to water the green roof on a varying seasonal schedule between 3:30 pm and 7:30 pm. Specifications for the two roofs in relation to their biodiversity, thermal and stormwater properties have been previously described in [44], [9] and [45], respectively.

2.2 Solar arrays

As construction was completed in 2019 and 2017 for the bio-solar and conventional roofs respectively, the two buildings used different solar panels. Along with other differences between buildings, this required that a series of corrections were made to the data to facilitate accurate comparisons between buildings.

The bio-solar roof employed 332 MAXEON 3 solar panels (SunPower, Australia; pNom 395W, efficiency 22.6%) and the conventional roof employed 346 NeON2 solar panels (LG, Australia; pNom 320W, efficiency 19.5%; see Supplementary Table 1 for full specifications). The bio-solar and conventional roofs amounted to 131.14 kWp and 110.72 kWp solar systems, respectively. Both buildings utilised four three-phase inverters (27.6k-AU000NNU2, SolarEdge, USA), rated to operate at 98% efficiency.

Prior to construction, each roof was modelled to estimate solar exposure, and the optimal panel layout. Building architects and solar engineers designed differences between panel layouts to account for the presence of the greenery in order to facilitate planting, maintenance and plant survival. On the bio-solar roof, solar panels were divided into several sections. The majority of panels (248) were situated above the main planted area, arranged with an azimuth of 0° (North-facing) and tilt angle of 15°. The remaining panels (84) were arranged between rooftop infrastructure, with an azimuth of 90° (East-facing), and a tilt angle of 2°. On average, the centre of the solar panels were 1 m above the substrate surface (~0.8

m above the leaf zone) due to consideration associated with promotion of plant growth and ease of maintenance.

The CSR did not have the same biological considerations as the green roof; hence the solar panels were arranged accordion-style, with the majority of panels arranged with an azimuth of 90° or 270° towards the centre of the roof space (145 East-facing and 145 West-facing). This layout was chosen by solar engineers to maximise sunlight exposure, as determined by modelling procedures prior to installation, similar to those presented in Section 2.3. Similar to the bio-solar roof, additional panels (56) were positioned between building infrastructure, with an identical layout to those towards the centre of the building. All panels utilised a tilt angle of 5° and were on average the centre of the panels were positioned 0.4 m above the concrete slab surface.

2.3 Solar modelling

Prior to analysis, a 3D model of the Barangaroo district was developed to estimate the average yearly incident solar irradiance on each rooftop (Figure 2) using the Rhino 6 modelling software (Rhino3D, USA) and DAYSIM in Grasshopper's Honeybee plug-in (Grasshopper3D, USA). Solar radiation calculations were based on the Sydney CBD Representative Meteorological Year (RMY) file (Sydney.947680, EnergyPlus, Australia). The model predicted the bio-solar roof would receive 6% more annual solar radiation than the conventional roof due to the reflectance and shading caused by the local urban geometries (Table 2, consideration 2).

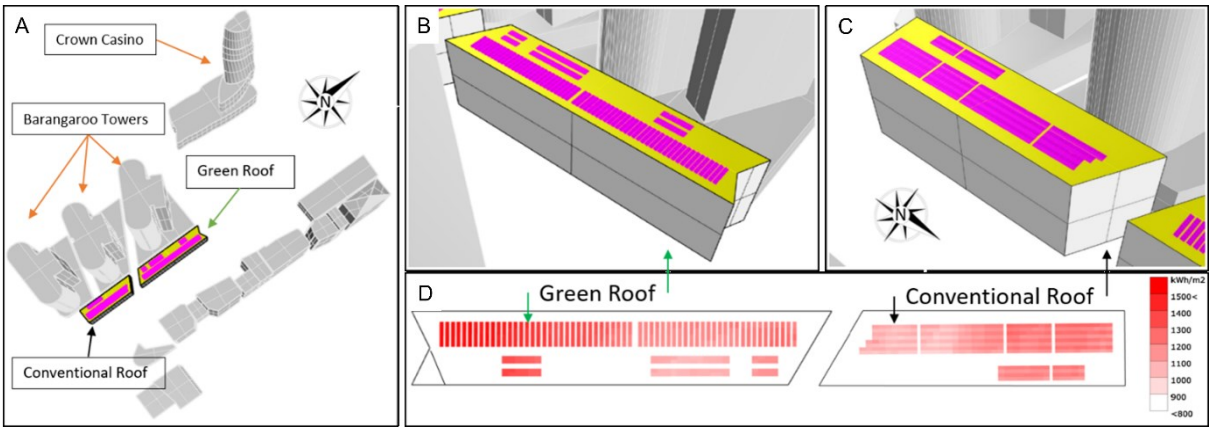

Figure 2. Rhino 6 3D model of; A) the Barangaroo district to determine the effect of urban geometries on reflectance and shading; B) the as-built bio-solar array; C) the conventional solar array; D) the average annual solar radiation received for each rooftop. Pink regions correspond to the panel layout for each roof, yellow regions represent the roof surface irrespective of plant/concrete coverage. Model dimensions are not to scale.

2.4 Data collection and corrections

Each solar array hosted a range of environmental sensors including ambient temperature and global horizontal irradiance (GHI). All environmental and solar data was uploaded to the SolarEdge monitoring platform for management. This monitoring platform could retrieve time-matched environmental measurements such as temperature from the local NSW Government weather station situated at Observatory Hill (Gauge 066062: approximate 590 linear meters).

Solar energy output data was collected from the SolarEdge monitoring web-platform on a fortnightly basis to coincide with on-site fortnightly onsite inspections. Solar energy outputs were collected for each inverter and summed each fortnight for both buildings. Rooftop pyranometers recorded GHI as the average hourly light intensity for each site.

Four corrections were applied to the gross energy output of the BSGR to account for differences between the two systems, resulting in a total reduction of the recorded energy output of ~19.8%. First, to account for differences in system capacity (BSGR: 131.14; CSR: 110.72 kWp), the BSGR output was reduced by ~15.54% (Table 1; Consideration 1). BSGR outputs were then reduced by a further 1.2% to account for losses associated with the age of the panels that were on CSR (Table 1; Consideration 5), and 3.1% to account for differences in panel efficiency (Table 1; Consideration 6). Output reductions for efficiency and age were based on the known differences or degradation rates of the two systems, as per the manufacturer specifications. Lastly, to account for differences in the temperature coefficients of the two systems (BSGR: -0.29%/1°C; CSR -0.38%/1°C above 25°C), BSGR energy outputs were reduced by 0.09%/°C for each 1°C panel temperatures were above 25°C (Table 1; Consideration 7) (See Supplementary Figure 1 for an infographic detailing these corrections).

As this study utilised the unique opportunity to analyse an *in-situ* commercial BSGR with a spatially unconfounded CSR of nearly identical size, two considerations involving convection air flow could not be addressed (Table 1; Considerations 8 and 9). Above and below panel convection could potentially influence the cooling potential of the system, and therefore energy output. However, both rooftops were modelled prior to construction, and for each roof the optimal layouts were chosen to maximise energy yield, along with facilitating planting, survival, and ease of maintenance of plant material on the BSGR. Therefore, while this study cannot quantify the effect of above and below panel convection, comparisons were made inclusive of these differences in roof design. It is likely that other commercial scale BSGRs would utilise panel designs based on these criteria. It is also known that in the surrounding region, most CSR solar arrays are designed similarly to the CSR in this study (based on satellite imagery).

Table 1. List of considerations and variance between buildings/solar arrays. Each consideration was either addressed (Yes), excluded (No) or randomised (N/A) based on the scope of the project. Specific issue is described in **bold** and the response in *italics.*

Considerations	Addressed	Comments
1. System Capacity	Yes	**The peak nominal power of each roof was different, with a variance in system size of 20.42 kWp (15.54%).** *Bio-solar roof energy output was reduced by ~15.54% to account for the difference between system sizes.*
2. Insolation: Shading	Yes	**Modules across and between roofs will experience shading differently due to urban geometries.** *Solar modelling was employed, and the observed performance was plotted against a standardised light profile through linear regression analysis. This aimed to achieve a standardised performance based on simulated light conditions within the confines of the seasonal light observed for each site.*
3. Insolation: Soiling	Yes	**Modules were impacted by soiling differently due to tilt, age and cleaning routines.** *Each roof was visually inspected fortnightly for the duration of the study and soiling was monitored. In instances where soiling was observed, building management organised cleaning which was conducted prior to the proceeding fortnight's inspection.*
4. Insolation: Array layout	Yes	**Module azimuth of each roof resulted in different insolation that PV panels were exposed to.** *Panel azimuth could not be changed for this study, however building architects and engineers consulted solar models to determine the optimal layout for each building with respect to the physical properties of each roof. Differences in azimuth and tilt were attributed by design teams to the specific physiological requirements of the green roof.*
5. Module: Degradation losses	Yes	**System age differed between roofs and the calculated efficiency of each system varied between manufacturers.** *The panel age difference between systems was accounted for by reducing the output of the panels on the green roof (~1.2%) for equivalence with the conventional roof.*
6. Module: Panel efficiency	Yes	**Module efficiency differed between solar arrays.** *The modules used on the green roof were rated 22.6% efficient compared to 19.6% on the conventional roof. As such, green roof outputs were reduced by ~3.1%.*
7. Module: Temperature coefficients	Yes	**Modules will respond to temperature fluctuations differently**. *The temperature coefficients of the BSGR and CSR modules were -0.29%/°C and -0.38%/°C, respectively for temperatures over 25°C. In instances where BSGR panel temperatures exceeded 25°C, output was reduced by the difference in temperature coefficients (0.09%/°C) to simulate output losses similar to the panels deployed on the conventional roof.*
8. Convection: Below panel	No	**Module azimuth (Green roof: North ballast layout; Conventional roof: East-West accordion layout) resulted in different convective heat transfer opportunities on the rear surface of the panels. Module temperatures will be impacted by this.** *The effect of convective heat transfer was not specifically addressed in this instance, and therefore the comparisons made can only be representative of the two solar arrays as built. Temperature variation of panels attributable to building design has been previously explored and directly linked to the function of the green roof through evapotranspiration* [9].
9. Convection: Above panel	No	**Module tilt (Green roof: 15° and 2°; Conventional roof: 5°) resulted in different convective heat transfer opportunities on the front surface of the panels. Module temperatures will be impacted by this.** *Module tilt could not be manipulated in this study and therefore convective heat transfer could not be equalised. Therefore, convective heat transfer owing to tilt was not assessed. The comparisons made are thus representative of the two solar arrays as built.*
10. Mismatch Losses	N/A	**No two modules will be electrically identical which incurs mismatch losses. These will limit the PV performance.** *Electrical mismatch losses are inherent in a multi-panel system. It is assumed in this study, and all studies on commercial systems, that mismatch losses would be randomly distributed across the roofs and any effects associated with panel mismatch were therefore be randomised within this design.*

2.5 Analysis

2.5.1 On-site measurements

Both solar exposure (expressed as GHI), as well as temperature were recorded locally for each roof. Both roofs were equipped with pyranometers, as well as ambient and panel temperature sensors. GHI was recorded for each building on a continuous timescale and averaged hourly. Both panel and ambient temperatures were recorded on a continuous

timescale and averaged hourly. All on-site data was collected weekly though the online SolarEdge monitoring platform.

2.5.2 Regression analysis

To determine the theoretical performance of each roof under a standardised lighting scenario, a multiple linear regression model was generated for hourly energy output using GHI, roof, and season as predictors. The model was as follows: Energy output (kWh) = (GHI × 0.0817) + (Bio-solar Roof × 0.978) + (Spring × 2.682) + (Summer × 2.009) + 0.613 (Intercept), with an R^2 of 0.90 ($p < 0.0001$) (R^2 or coefficient of determination represents the proportion of variance in energy output that is explained by the predictors of the model, on a scale of 0-1). The model output was then used to compare the estimated performance of each roof under standardised on-site conditions. Input GHI spanned from 25 W/m^2 (minimum daytime irradiance) to the maximum shared irradiance for both roofs per season (745, 796, and 752 W/m^2 for Spring, Summer and Autumn respectively). Results were deemed significant at $\alpha = < 0.05$ (α or significance level represents the probability of the analysis yielding a Type I error, that is the risk of a false-positive result).

2.5.3 Alternative performance metrics

In addition to energy production, solar systems are often described in respect to their economic and environmental/social benefits. In this sense, the energy outputs of both buildings can be described in relation to the energy savings in dollars, as well as the mitigation of e-CO_2 (carbon dioxide equivalent greenhouse gasses) emissions related to the use of renewable energy as opposed to energy from a fossil fuel powered grid. Additionally, plant matter on a green roof could also contribute to the removal of ambient CO_2 through photosynthesis and biomass growth, with the total CO_2 removal/mitigation being relatable to the CO_2 abatement from planting of urban trees.

To calculate the financial value generated through the use of the solar arrays on each building, the net output of each roof was multiplied by the retail energy costs (AUD $317.5 MWh) as described by the Australian Energy Regulator (AER) for the time period [46]. The mitigation of greenhouse gas emissions was calculated using the NSW National Greenhouse Accounts Factor of 0.81 kg e-CO2/kWh [47], and the CO_2 removal potential of the plant material on the bio-solar roof was estimated according to Shafique et al., [48]. A translation of clean energy produced to “trees planted” equivalents was calculated using the ratio of 0.0117:1 trees per kWh as outlined by US EPA [49].

3. Results and Discussion

3.1 Observed difference between Bio- and Conventional solar

The Rhino 3D solar model predicted an annual GHI exposure difference between the BSGR and CSR of 6% due to surrounding buildings both blocking and reflecting light. However, during the 237 days of this study, the measured light exposure was both greater than the Rhino model predicted, and varied significantly between seasons. On average, the BSGR received 4.37 and 61.31% more GHI than the CSR in Spring and Autumn respectively, whilst receiving 5.67% less GHI in Summer (Figure 3A). While the current analysis did not incorporate the Winter months, or the full date range of Spring, the observed solar exposure was more than double (15.72%) that predicted by the Rhino 3D predictive model. It is therefore evident that conducting on-site monitoring for environmental variables such as GHI and temperature, which are two key factors in solar energy outputs, are paramount for these types of assessments.

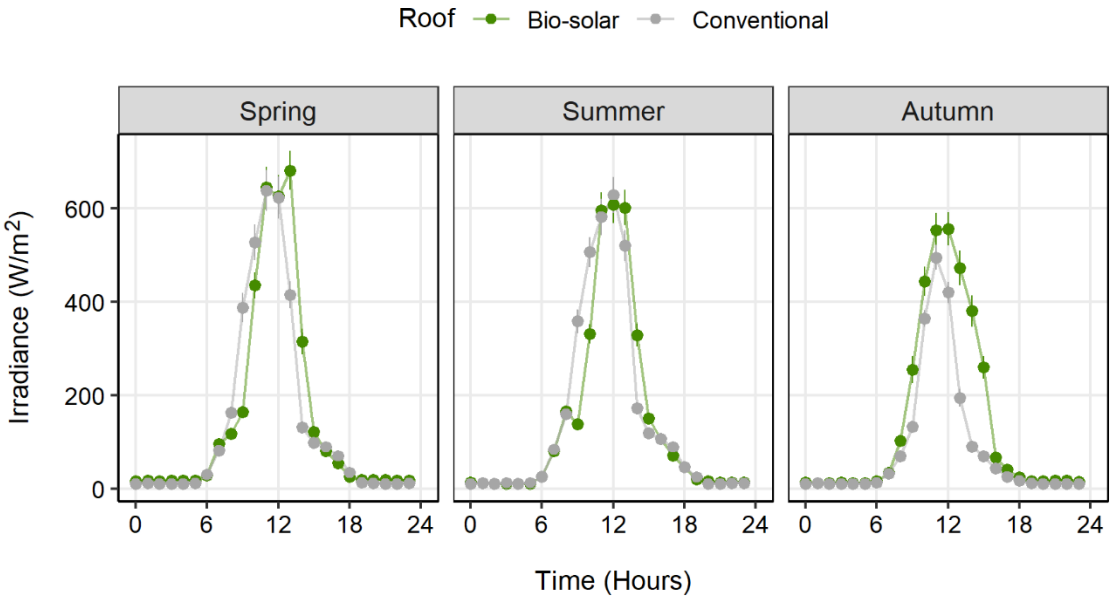

Figure 3. Mean ± SEM hourly GHI reported by on-site pyranometers during each season for both roofs. Within season variance in light availability are largely attributed to urban geometries, and between season variance to seasonal day-arc. During Spring and Autumn, the BSGR received an average of 4.37% and 61.31% more GHI than the CSR, however in Summer the CSR received an average of 5.67% more GHI than the BSGR.

For the duration of this study, the BSGR maintained an average ambient temperature 1.00, 1.12 and 0.72°C cooler than the CSR (Figure 4A) for Spring, Summer and Autumn respectively. However, during peak GHI hours (11 am-2 pm inclusive (Figure 3)), the BSGR ambient temperatures were only 0.44, 0.95 and 0.26°C cooler than the CSR (Figure 4A). Despite ambient roof temperature not being substantially different between buildings, a previous study conducted by Fleck et al., [9] on the same two roofs found a significant difference between the two rooftop microclimates (the temperature gradient ~1m from the surface of the roof/plant foliage). One unexplored aspect from this previous study was the potential cooling effect of the BSGR on the solar array. Below-panel temperatures were up to 6 and 11°C cooler on the BSGR than the CSR during Spring and Summer, respectively. In this study

however we observed a substantial reduction in solar panel temperature during peak GHI hours, which aligns with the previously reported below-panel temperatures [9]. This effect is more likely due to the evapotranspiration and reduced latent heat/solar reflectance of the plant material than panel orientation, where plant foliage may apply a foliage-specific drag coefficient [50], slowing or reducing the total airflow beneath panels, and thus reducing the effect of below-panel convection to some degree. However, as this was not specifically measured in the current study the effect of below-panel convection cannot be excluding as a contributing factor.

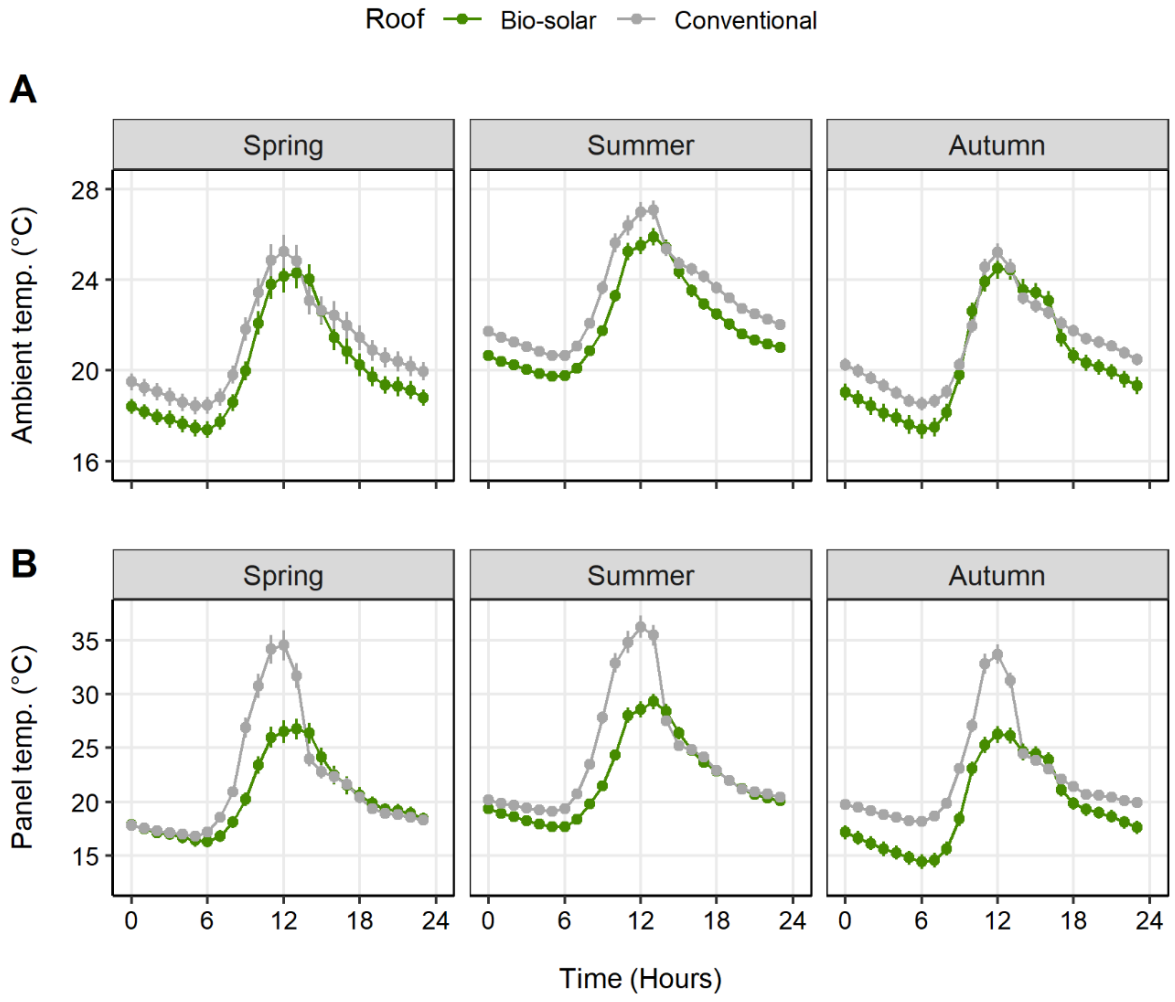

Figure 4. Mean ± SEM hourly ambient (A) and panel temperatures (B) reported by on-site temperature sensors during each season for both roofs. The ambient rooftop and panel temperatures of the BSGR were on average 1.00, 1.12 and 0.72°C and 1.50, 2.10 and 2.88°C cooler than the CSR in Spring, Summer, and Autumn, respectively. During peak GHI hours (11:00 to 14:00 inclusive), ambient and panel temperatures on the BSGR was on average 0.44, 0.95 and 0.26°C and 4.68, 4.95 and 4.98°C cooler than the CR in Spring, Summer and Autumn, respectively.

The BSGR panel temperatures were 1.50, 2.10 and 2.88°C cooler than those on the CSR in Spring, Summer and Autumn, respectively, however during peak GHI hours, the BSGR was 4.68, 4.95 and 4.98°C cooler for the same time period (Figure 4B). These temperature reductions are significant as solar panel performance decreases above 25°C [40]. In this study, the temperature coefficients of the BSGR and CSR were -0.29 and -0.38% for each 1°C above 25°C. It is therefore evident that the BSGR was able to mitigate performance loss due to

temperature by 1.36, 1.44 and 1.44% during peak GHI hours in Spring, Summer and Autumn respectively.

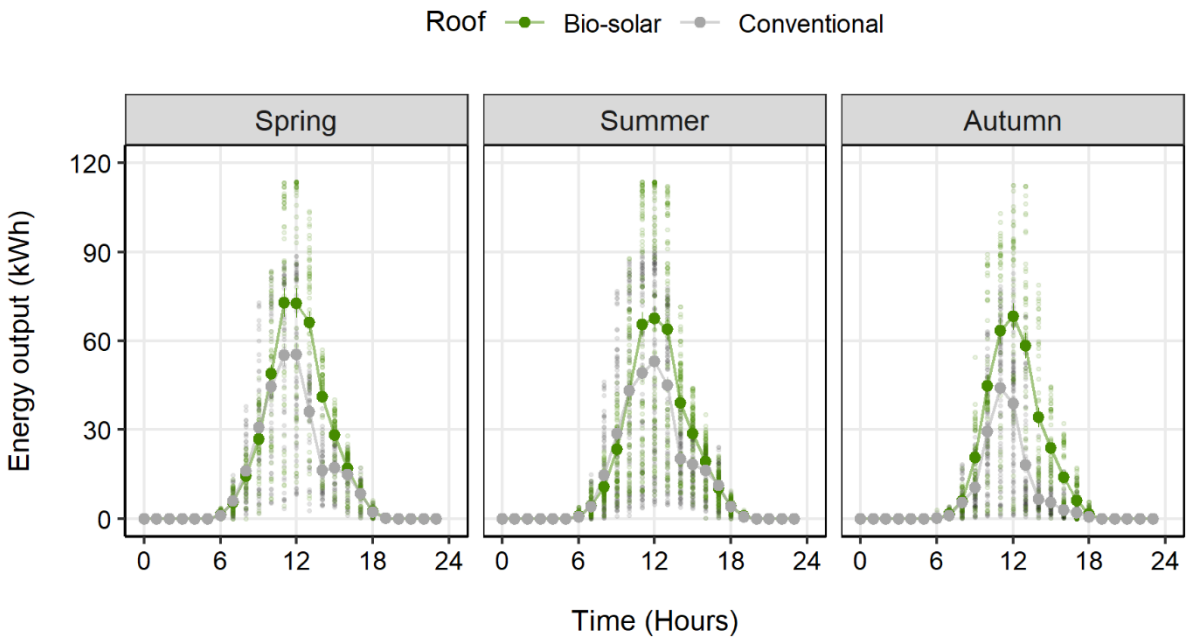

Figure 5. Mean ± SEM hourly energy output (kWh) during each season for both roofs. The BSGR generated an average 32.52, 21.25 and 107.29% more kWh than the CSR during Spring, Summer and Autumn respectively. Differences between BSGR and CSR maximum power outputs were 25.14, 20.35 and 29.8 kWh for Spring, Summer and Autumn respectively.

For each season, the average hourly energy output for the BSGR was 16.85 ± 0.76 (SEM), 15.66 ± 0.58 and 14.30 ± 0.74 kWh, whereas the CSR outputs were 12.71 ± 0.58, 12.92 ± 0.48 and 6.90 ± 0.32 kWh (Figure 5), although it appears that these performance differences are predominantly driven by solar exposure (Figure 3). However, despite the variance in GHI exposure between seasons, and the clear effect of the urban geometry (which can be seen in Fig 3: Spring; 8 am-10 am and 1 pm-3 pm, Summer; 9 am-11 am and 1 pm-3 pm, Autumn; 8 am-3 pm), in instances where the solar exposure was approximately equal, the energy output of the BSGR was substantially higher than the CSR. The BSGR produced an average of 17.71 and 17.32 (Spring), and 16.45 and 14.47 (Summer) kWh more energy than the CSR (Figure 5) at 11 am and 12 pm, respectively. This was likely due to differences in panel temperature, caused by the evapotranspiration effect of the BSGR and the resulting cooler microclimate [9,51] (Figure 4A and B). Differences in solar irradiance aside (Figure 3), the BSGR in this study had a LAI of 4.35, which would likely have increased the cooling potential of the BSGR to a higher degree than those BSGRs studied previously [38,52]. However, due to the discrepancies in solar exposure, it is difficult to isolate the primary causative effect for the increased energy output of the BSGR, where the BSGR produced an average of 32.52, 21.25 and 107.29% more energy for Spring, Summer, and Autumn, respectively (Figure 5). As such, the observed system performance of both systems was modelled under standardised lighting conditions to eliminate the effect of the increased solar exposure recorded on the BSGR.

3.2 Modelled difference between Bio-solar and Conventional solar

To eliminate variability caused by the effect of urban geometries and seasonal day arc, a multiple linear regression model was employed using GHI, roof and season as predictors (Figure 6). Under standardised lighting scenarios, the BSGR outperformed the CSR by 4.14, 4.16 and 5.21% for Spring, Summer and Autumn, respectively. For the duration of the study, on average, the BSGR produced 4.5% more energy than the CSR at any given light level.

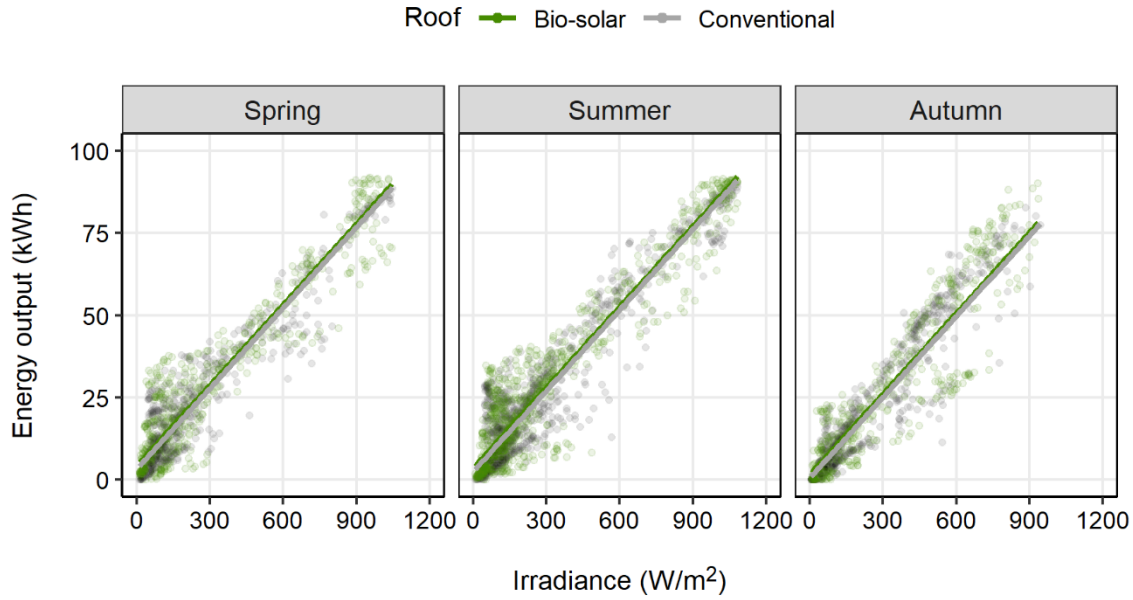

Figure 6. Daytime irradiance versus energy output reported by on-site sensors during each season for both roofs. Lines depict fitted multiple linear regression model: Energy output (kWh) = (GHI × 0.0817) + (BSGR × 0.978) + (Spring × 2.682) + (Summer × 2.009) + 0.613 (Intercept) with $R^2 = 0.90$ ($p < 0.0001$).

Previous literature comparing PV system performance varies in the metrics by which system efficiencies have been reported, with authors reporting either total energy output for a given period, or the average difference in system performance for a specified period (Table 2). Most studies have been conducted on small experimental or pilot scale systems, with few testing *in-situ* commercial scale BSGRs with the appropriate controls. The performance differences presented here are higher than those previously reported from both experimental and pilot scale studies BSGR (Table 2).

The study that achieved the closest average system performance to ours was conducted by Hui and Chan [35] in Hong Kong (Köppen climate type Cfa), who reported a 4.3% increase in performance by a BSGR when compared to an internal control roof. This study used simulations and modelling to estimate the performance increase of a commercial BSGR, reporting an increase of 8.3% in the total energy output compared to a simulated CSR [35]. While the average performance difference between Hui and Chan's study and the efficiencies reported here are similar, the total energy produced varies substantially.

Table 2. Comparison of previous literature to this study in respect to; study location, Köppen climate classification, study type, study duration, bio-solar array size/panel coverage (m^2), comparison made, and difference in solar energy output between treatments. Results are reported as total energy output (tot) or average difference in system performance (sys).

Study	Location	Köppen	Type	Duration	Size	Comparison	Result
This study	***Sydney, Australia***	***Cfa***	***Experimental & Simulation***	***8 months (237 days)***	***593.96 m^2***	***Commercial bio-solar vs independent conventional PV***	***4.5% (sys) 23.83% (tot)***
Nagengast et al., [53]	Pittsburgh, USA	Cfa	Experimental & Simulation	16 months	87 m^2	Model bio-solar vs internal PV-black roof	0.8-1.5% (tot)
Köhler et al., [54]	Germany	Cfb	Pilot Experiment	12 months	Undisclosed	Variable model bio-solar vs internal PV-bitumen roofs	6.5% (tot)
Perez et al., [39]	New York City, USA	Cfa	Pilot Experiment & Simulation	10 months	Undisclosed	Bio-solar vs internal PV gravel	2.42% (tot)
Hui & Chan, [35]	Hong Kong	Cfa	Pilot Experiment & Simulation	1 days 12 months	Undisclosed *2,494 m^2*	Bio-solar vs internal conventional PV	4.3% (sys) 8.3% (tot)
Chemisana & Lamnatou, [38]	Spain	BSk	Pilot Experiment	5 days	1.69 m^2	Model bio-solar vs internal PV gravel	1.29-3.33% (tot)
Osma-Pinto & Ordóñez-Plata [55]	Colombia	Af	Pilot Experiment	Undisclosed	15 m^2	Model bio-solar vs internal PV-black roof	0.9-1.7% (sys)
Ogaili & Sailor, [11]	Portland, USA	Csb	Pilot Experiment	3 months	6.6 m^2	Model bio-solar vs internal PV-black/white roof	0.8-1.2% (sys)
Alshayeb & Chang, [37]	Kansas, USA	BSk	Pilot Experiment	12 months	14.7 m^2	Model bio-solar vs internal PV-black roof	3.3% (sys) 1.4% (tot)
Kaewpraek et al, [56]	Thailand	Am	Pilot Experiment	1 months	13.58 m^2	Model bio-solar vs internal PV-grey roof	2% (sys) 5% (tot)

Differences between previous findings and the results presented here may be influenced by study duration or plant selection. For many studies ([53], [54], [39], [37]), the inclusion of the winter months may have reduced the difference in system performance either due to the cooler weather reducing the impact of the BSGR, or reduced solar exposure reducing the performance of both systems. It is potentially possible that the inclusion of winter months in the current study would have also reduced the average system performance and possibly the total energy output difference. However, for the Spring, Summer and Autumn months, our reported average efficiencies are higher than previously reported. Additionally, many past studies have utilised plants from the genus *Sedum* for their experimental BSGRs [35,38]. This Crassulacean species has substantially lower LAI and practical planting densities [44] than many commercial *in-situ* systems, such as the one tested in the current study. A higher LAI and planting density would substantially increase the evapotranspiration effect, reduce latent heat, and increase the solar reflectance of the BSGR [40,41], thus improving the thermal regulation properties of the space [57].

It is therefore plausible that the installation and use of BSGRs in similar regions and climates of the world to the current work would stand to gain substantial increases in electrical energy generation BSGR, as well as benefit from the numerous additional services that BSGRs provide to building occupants. As such, while the results presented here are directly representative of the Eastern Australian coast and similar Cfa climates, the quantified benefits of a BSGR to provide a cooler microclimate for sustained increases in solar energy output can be applied globally.

3.3 Alternative Performance Metrics

For the period observed, the BSGR and CSR produced 74.05 and 59.80 MWh of renewable energy, with the BSGR producing 23.83% more energy than the CSR. Based on the retail consumer market price outlined by the AER [46], the BSGR and CSR offset the purchase price of energy by $23,511.52 and $18,985.29 AUD, respectively. The implementation of a green roof therefore served to increase the economic benefits of the solar array by 23.84**%** ($4,526.22 AUD; Figure 7).

While these values may appear small when compared to the scale and capital cost of the two commercial systems tested, there is a significant push by governments worldwide for the adoption of localised renewable energy within urban environments [58]. In the short term, it is expected that the financial savings gained through the use of a solar or bio-solar roof would increase from what was observed here due to growing insecurities in the energy market, especially in countries with unstable energy markets [59].

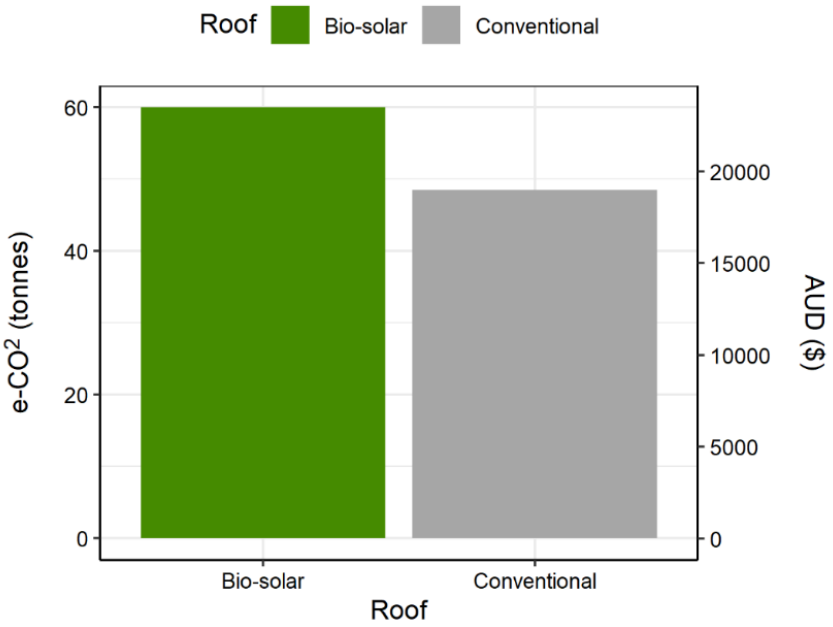

Figure 7. Performance difference between BSGR and CSR using alternative metrics. Axis-Y1 demonstrates the e-CO_2 mitigation of each system (BSGR; 59.98 t e-CO_2, CSR; 48.43 t e-CO_2), and Axis-Y2 demonstrates the price offset (BSGR; $23,511.52, CSR; $18,985.29, in $AUD) of each system. The BSGR and CSR roofs are represented in green and grey, respectively.

Based on the total energy generated by each roof, the bio-solar and conventional roofs were able to mitigate greenhouse gas (GHG) emissions of 59.98 and 48.43 t e-CO_2 respectively, based on the Australian National Greenhouse Accounts Factor (NGAF) [47]. The increase in bio-solar energy production equates to an e-CO_2 offset of 11.55 t greater than that associated with the conventional roof (Figure 7). These GHG emission calculations are based on the consumption of purchased electricity or loss from the grid, and therefore localised energy generation for each building would offset these emissions by reducing reliance on the grid. Additionally, the bio-solar roof hosted over 15,000 individual plants, which innately remove CO_2 from the atmosphere through photosynthesis during growth. Estimates derived from the literature [48,60] suggest that the green-components of the BSGR could have removed up to

1.56 t of CO_2 from the atmosphere and stored this carbon in the form of biomass gain over the duration of the study (237 days). This would increase the e-CO_2 mitigation potential of a similarly sized bio-solar roof to 13.10 t for the same period. Colloquially, the mitigation of GHG emissions is often reported as an equivalent to number of "trees planted". Here we observe equivalent tree plantings of 866.41 and 699.62 trees for the bio-solar and conventional roofs, respectively. With the inclusion of the photosynthetic removal of atmospheric carbon, the BSGR has an equivalent carbon capture/abatement to planting 192.49 urban trees and growing them for 10 years.

The inclusion of photosynthetic removal of atmospheric CO_2 in the calculation of GHG mitigation potential of green and bio-solar roofs will, however, be reduced by biomass management by green roof maintenance. The removal of atmospheric CO_2 through photosynthesis is primarily driven by biomass accumulation, both above and below ground [61]. However, for commercial green roofs, maintenance is usually performed whereby plant material is maintained at certain heights, especially when grown around solar modules. The removal of plant biomass, and the disposal of plant material will largely determine the CO_2 removal potential of a green roof, where biomass burning or composting will lead to the reemission of a proportion of the stored carbon [62]. Additionally, some carbon is sequestered by the plant roots into the substrate, and made available to rhizospheric microbes [61], and thus transferred to the substrate's labile carbon pool. From the labile carbon pool, there is the potential for microbial biomass to consume this carbon and respire or emit volatile organic compounds back into the atmosphere [61,63]. It is therefore essential that further research be conducted on how green and bio-solar roof biomass management will affect the carbon sequestration potential of this promising technology.

Lastly, a factor unexplored here that would serve to increase the e-CO_2 emission performance of bio-solar roofs is the inherent ability of green and bio-solar roofs to insulate buildings [9,48,63]. The thermal insulation effect of green and bio-solar roofs has been shown in experimental studies to have the potential to reduce annual building energy consumption by 15.1% in warm Mediterranean climates [64]. To date, few studies have successfully determined the energy saving potential of green and bio-solar roofs from experimental studies on commercial systems, and it is therefore recommended that further research be conducted on medium-large scale commercial projects to determine this effect across a range of climates.

4. Conclusions

Here we present the largest known commercial BSGR solar energy study to date. BSGR average energy output was 4.5% greater than the CSR, and the total energy output was 23.83% higher. The BSGR served to reduce the greenhouse gas emissions of the building through off-setting fossil fuel powered energy consumption by an additional 11.55 t e-CO_2, with the potential for up to 1.55 t of additional CO_2 being mitigated by the plants on the roof. This increase in energy output equates to $4,526.22 AUD and an equivalent of 192.49 "trees planted" and grown over 10 years in an urban setting. The inclusion of a green roof over a

conventional solar array served to increase the energy output of the system by 23.88 kWh, reduce the GHG emissions by 0.019 t e-CO2 and produced an additional $7.62 AUD per m^2 of solar panels deployed for the duration of the study. The effect of the BSGR during the winter months, however, is unknown, and it is therefore recommended that future studies along the Eastern Australian coastline, or similar climates, conduct long term monitoring studies on *in-situ* commercial scale BSGRs and CSRs.

Declaration of competing interest

The authors declare that they have no known competing financial interests or personal relationships that could have appeared to influence the work reported in this paper.

Acknowledgements

This work was funded through the City of Sydney grants and sponsorship program: Environmental Performance – Innovation Grant 2019-2020 (2020/037855/ EPI R3 201920005). This work was further supported by LendLease Pty Ltd and Junglefy Pty Ltd for in-kind contributions and facilitating site access.

The authors would like to acknowledge the efforts of Mr. Giovanni Cercone, Mr. Martino Masini and Mr. Luke Brown for facilitating access to International Towers. The authors would like to further acknowledge the efforts of Miss Angela Begg, Mr. Graham Carter, Mr. Peter Zacharia and Mr. Peter Flynn of LendLease P/L for their support and supply of the Rhino 3D solar model for site-wide light exposure, as well as information regarding solar-array modelling, design and layout.

Most of all, the authors would like to thank Lucy Sharman, Sustainability Manager for LendLease P/L, without whose management, direction, and facilitation this project would have not been possible.

References

[1] O. Schneising, M. Reuter, M. Buchwitz, J. Heymann, H. Bovensmann, J.P. Burrows, Terrestrial carbon sink observed from space: variation of growth rates and seasonal cycle amplitudes in response to interannual surface temperature variability, Atmos. Chem. Phys. 14 (2014) 133–141. https://doi.org/10.5194/acp-14-133-2014.

[2] Intergovernmental Panel on Climate Change, Climate Change 2014: Mitigation of Climate Change, Cambridge University Press, 2015. https://doi.org/10.1017/CBO9781107415416.

[3] L. Pérez-Lombard, J. Ortiz, C. Pout, A review on buildings energy consumption information, Energy Build. 40 (2008) 394–398. https://doi.org/10.1016/j.enbuild.2007.03.007.

[4] D. Gielen, F. Boshell, D. Saygin, M.D. Bazilian, N. Wagner, R. Gorini, The role of renewable energy in the global energy transformation, Energy Strateg. Rev. 24 (2019) 38–50. https://doi.org/10.1016/j.esr.2019.01.006.

[5] S. Sorrell, Reducing energy demand: A review of issues, challenges and approaches, Renew. Sustain. Energy Rev. 47 (2015) 74–82. https://doi.org/10.1016/j.rser.2015.03.002.

[6] T.N. Thanh, P.V. Minh, K.D. Trung, T. Do Anh, Study on performance of rooftop solar power generation combined with battery storage at office building in northeast region, vietnam, Sustain. 13 (2021). https://doi.org/10.3390/su131911093.

[7] M. Fadzli Haniff, H. Selamat, R. Yusof, S. Buyamin, F. Sham Ismail, Review of HVAC scheduling techniques for buildings towards energy-efficient and cost-effective operations, Renew. Sustain. Energy Rev. 27 (2013) 94–103. https://doi.org/10.1016/j.rser.2013.06.041.

[8] M. Taleghani, Outdoor thermal comfort by different heat mitigation strategies- A review, Renew. Sustain. Energy Rev. 81 (2018) 2011–2018. https://doi.org/10.1016/j.rser.2017.06.010.

[9] R. Fleck, R.L. Gill, S. Saadeh, T. Pettit, E. Wooster, F. Torpy, P. Irga, Urban green roofs to manage rooftop microclimates: A case study from Sydney, Australia, Build. Environ. 209 (2022) 108673. https://doi.org/10.1016/j.buildenv.2021.108673.

[10] L. Smalls-Mantey, F. Montalto, The seasonal microclimate trends of a large scale extensive green roof, Build. Environ. 197 (2021) 107792. https://doi.org/10.1016/j.buildenv.2021.107792.

[11] H. Ogaili, D.J. Sailor, Measuring the Effect of Vegetated Roofs on the Performance of Photovoltaic Panels in a Combined System, J. Sol. Energy Eng. Trans. ASME. 138 (2016) 1–8. https://doi.org/10.1115/1.4034743.

[12] M. Razzaghmanesh, S. Beecham, The hydrological behaviour of extensive and intensive green roofs in a dry climate, Sci. Total Environ. 499 (2014) 284–296. https://doi.org/10.1016/j.scitotenv.2014.08.046.

[13] J. Yang, Q. Yu, P. Gong, Quantifying air pollution removal by green roofs in Chicago, Atmos. Environ. 42 (2008) 7266–7273. https://doi.org/10.1016/j.atmosenv.2008.07.003.

[14] J. Yang, Z.H. Wang, Physical parameterization and sensitivity of urban hydrological models: Application to green roof systems, Build. Environ. 75 (2014) 250–263. https://doi.org/10.1016/j.buildenv.2014.02.006.

[15] C.Y. Jim, S.W. Tsang, Biophysical properties and thermal performance of an intensive green roof, Build. Environ. 46 (2011) 1263–1274. https://doi.org/10.1016/j.buildenv.2010.12.013.

[16] D.B. Rowe, K.L. Getter, The role of extensive green roofs in sustainable development, HortScience. 41 (2006) 1276–1285.

[17] M. Shafique, R. Kim, M. Rafiq, Green roof benefits, opportunities and challenges – A review, Renew. Sustain. Energy Rev. 90 (2018) 757–773. https://doi.org/10.1016/j.rser.2018.04.006.

[18] B.A. Currie, B. Bass, Estimates of air pollution mitigation with green plants and green roofs using the UFORE model, Urban Ecosyst. 11 (2008) 409–422. https://doi.org/10.1007/s11252-008-0054-y.

[19] D. Suszanowicz, A. Kolasa-Więcek, The impact of green roofs on the parameters of the environment in urban areas-review, Atmosphere (Basel). 10 (2019). https://doi.org/10.3390/ATMOS10120792.

[20] T. Van Renterghem, D. Botteldooren, Reducing the acoustical façade load from road traffic with green roofs, Build. Environ. 44 (2009) 1081–1087. https://doi.org/10.1016/j.buildenv.2008.07.013.

[21] T. Van Renterghem, D. Botteldooren, In-situ measurements of sound propagating over extensive green roofs, Build. Environ. 46 (2011) 729–738. https://doi.org/10.1016/j.buildenv.2010.10.006.

[22] T. Van Renterghem, M. Hornikx, J. Forssen, D. Botteldooren, The potential of building envelope greening to achieve quietness, Build. Environ. 61 (2013) 34–44. https://doi.org/10.1016/j.buildenv.2012.12.001.

[23] F. Mayrand, P. Clergeau, Green roofs and greenwalls for biodiversity conservation: A contribution to urban connectivity?, Sustain. 10 (2018). https://doi.org/10.3390/su10040985.

[24] S.E. Clemants, J. Marinelli, G. Moore, E. Peters, N. Dunne, J. Blackburn, B. Botanic, G. Website, A. Dorfman, D. Allen, Green Roofs and Biodiversity, Urban Habitats. 4 (2006) 1–26. http://www.urbanhabitats.org/v04n01/urbanhabitats_v04n01_pdf.pdf.

[25] R. Fioretti, A. Palla, L.G. Lanza, P. Principi, Green roof energy and water related performance in the Mediterranean climate, Build. Environ. 45 (2010) 1890–1904. https://doi.org/10.1016/j.buildenv.2010.03.001.

[26] J. Mentens, D. Raes, M. Hermy, Green roofs as a tool for solving the rainwater runoff problem in the urbanized 21st century?, Landsc. Urban Plan. 77 (2006) 217–226. https://doi.org/10.1016/j.landurbplan.2005.02.010.

[27] K. Vijayaraghavan, F.D. Raja, Design and development of green roof substrate toimprove runoff water quality: Plant growth experiments and adsorption, Water Res. 63 (2014) 94–101. https://doi.org/10.1016/j.watres.2014.06.012.

[28] X. Zheng, Y. Zou, A.W. Lounsbury, C. Wang, R. Wang, Green roofs for stormwater runoff retention: A global

quantitative synthesis of the performance, Resour. Conserv. Recycl. 170 (2021) 105577. https://doi.org/10.1016/j.resconrec.2021.105577.
[29] R.C. Feitosa, S.J. Wilkinson, Attenuating heat stress through green roof and green wall retrofit, Build. Environ. 140 (2018) 11–22. https://doi.org/10.1016/j.buildenv.2018.05.034.
[30] R.C. Feitosa, S.J. Wilkinson, Small-scale experiments of seasonal heat stress attenuation through a combination of green roof and green walls, J. Clean. Prod. 250 (2020) 119443. https://doi.org/10.1016/j.jclepro.2019.119443.
[31] C. Rosenzweig, W. Solecki, L. Parshall, S. Gaffin, B. Lynn, R. Goldberg, J. Cox, S. Hodges, Mitigating New York City's heat island with urban forestry, living roofs, and light surfaces, in: 86th AMS Annu. Meet., 2006.
[32] K.R. Smith, P.J. Roebber, Green roof mitigation potential for a proxy future climate scenario in Chicago, Illinois, J. Appl. Meteorol. Climatol. 50 (2011) 507–522. https://doi.org/10.1175/2010JAMC2337.1.
[33] R. Ciriminna, F. Meneguzzo, M. Pecoraino, M. Pagliaro, Solar Green Roofs: A Unified Outlook 20 Years On, Energy Technol. 7 (2019) 1–7. https://doi.org/10.1002/ente.201900128.
[34] Z. Zhang, C. Szota, T.D. Fletcher, N.S.G. Williams, J. Werdin, C. Farrell, Influence of plant composition and water use strategies on green roof stormwater retention, Sci. Total Environ. 625 (2018) 775–781. https://doi.org/10.1016/j.scitotenv.2017.12.231.
[35] S.C.M. Hui, S.C. Chan, Integration of green roof and solar photovoltaic systems, in: Jt. Symp. 2011 Integr. Build. Des. New Era Sustain., 2011: pp. 1–12.
[36] S.E. Ouldboukhitine, R. Belarbi, I. Jaffal, A. Trabelsi, Assessment of green roof thermal behavior: A coupled heat and mass transfer model, Build. Environ. 46 (2011) 2624–2631. https://doi.org/10.1016/j.buildenv.2011.06.021.
[37] M.J. Alshayeb, J.D. Chang, Variations of PV panel performance installed over a vegetated roof and a conventional black roof, Energies. 11 (2018). https://doi.org/10.3390/en11051110.
[38] D. Chemisana, C. Lamnatou, Photovoltaic-green roofs: An experimental evaluation of system performance, Appl. Energy. 119 (2014) 246–256. https://doi.org/10.1016/j.apenergy.2013.12.027.
[39] M.J.R. Perez, N.T. Wight, V.M. Fthenakis, C. Ho, Green-roof integrated pv canopies-an empirical study and teaching tool for low income students in the South Bronx, in: World Renew. Energy Forum, WREF 2012, Incl. World Renew. Energy Congr. XII Color. Renew. Energy Soc. Annu. Conf., 2012: pp. 4046–4052.
[40] L. Bianco, V. Serra, F. Larcher, M. Perino, Thermal behaviour assessment of a novel vertical greenery module system: first results of a long-term monitoring campaign in an outdoor test cell, Energy Effic. 10 (2017) 625–638. https://doi.org/10.1007/s12053-016-9473-4.
[41] M.G. Gomes, C.M. Silva, A.S. Valadas, M. Silva, Impact of vegetation, substrate, and irrigation on the energy performance of green roofs in a Mediterranean climate, Water (Switzerland). 11 (2019). https://doi.org/10.3390/w11102016.
[42] A. Brambilla, E. Gasparri, Hygrothermal behaviour of emerging timber-based envelope technologies in Australia: A preliminary investigation on condensation and mould growth risk, J. Clean. Prod. 276 (2020) 124129. https://doi.org/10.1016/j.jclepro.2020.124129.
[43] Bureau of Meteorology, Bureau of Meteorology, Aust. Gov. (2021). bom.gov.au/nsw.
[44] E.I.F. Wooster, R. Fleck, F. Torpy, D. Ramp, P.J. Irga, Urban green roofs promote metropolitan biodiversity: A comparative case study, Build. Environ. 207 (2022) 108458. https://doi.org/10.1016/j.buildenv.2021.108458.
[45] R. Fleck, M.T. Westerhausen, N. Killingsworth, J. Ball, F.R. Torpy, P.J. Irga, The hydrological performance of a green roof in Sydney, Australia: A tale of two towers, Build. Environ. (2022) 109274. https://doi.org/10.1016/j.buildenv.2022.109274.
[46] AER, Annual retail markets report 2019–20, 2020.
[47] DISER, National Greenhouse Accounts Factors October 2020, 2020. https://www.industry.gov.au/data-and-publications/national-greenhouse-accounts-factors-2020.
[48] M. Shafique, X. Xue, X. Luo, An overview of carbon sequestration of green roofs in urban areas, Urban For. Urban Green. 47 (2020) 126515. https://doi.org/10.1016/j.ufug.2019.126515.
[49] Greenhouse Gas Equivalencies Calculator, United States Environ. Prot. Agency. (2021).
[50] V. Etminan, R.J. Lowe, M. Ghisalberti, A new model for predicting the drag exerted by vegetation canopies, Water Resour. Res. 53 (2017) 3179–3196. https://doi.org/10.1002/2016WR020090.
[51] C. Lamnatou, D. Chemisana, A critical analysis of factors affecting photovoltaic-green roof performance, Renew. Sustain. Energy Rev. 43 (2015) 264–280. https://doi.org/10.1016/j.rser.2014.11.048.
[52] T. Baumann, H. Nussbaumer, M. Klenk, A. Dreisiebner, F. Carigiet, F. Baumgartner, Photovoltaic systems with vertically mounted bifacial PV modules in combination with green roofs, Sol. Energy. 190 (2019) 139–146. https://doi.org/10.1016/j.solener.2019.08.014.
[53] A.L. Nagengast, C. Hendricksen, H.S. Matthews, Energy Performance Impacts from Competing Low-slope Roofing Choices and Photovoltaic Technologies, 2012. http://search.proquest.com/docview/1313752974?accountid=14556%5Cnhttp://vv6tt6sy5c.search.serialssolutions.com/?ctx_ver=Z39.88-2004&ctx_enc=info:ofi/enc:UTF-8&rfr_id=info:sid/ProQuest+Dissertations+%26+Theses+Global&rft_val_fmt=info:ofi/fmt:kev:mtx:disser.
[54] M. Kohler, R. Feige, W. Wiartalla, Interaction between PV-systems and extensive green roofs, in: 5th Annu. Int. Green. Rooftops Sustain. Communities Conf. Award. Trade Show, Green Roofs for Healthy Cities, Minneapolis, 2007.
[55] G. Osma-Pinto, G. Ordóñez-Plata, Measuring factors influencing performance of rooftop PV panels in warm

tropical climates, Sol. Energy. 185 (2019) 112–123. https://doi.org/10.1016/j.solener.2019.04.053.
[56] C. Kaewpraek, L. Ali, M.A. Rahman, M. Shakeri, M.S. Chowdhury, M.S. Jamal, M.S. Mia, J. Pasupuleti, L.K. Dong, K. Techato, The effect of plants on the energy output of green roof photovoltaic systems in tropical climates, Sustain. 13 (2021) 1–10. https://doi.org/10.3390/su13084505.
[57] E. Grala da Cunha, C. Maria Brito Correa, R. Peil, V. Mülech Ritter, D. Hohn, H. Maieves, J. Neila González, M. Estima Silva, R. Karini Leitzke, Characterizing leaf area index of rooftop farm to assess thermal-energy performance by simulation, Energy Build. 241 (2021) 110960. https://doi.org/10.1016/j.enbuild.2021.110960.
[58] City of Sydney, Greening Sydney Strategy, 2021. https://www.cityofsydney.nsw.gov.au/-/media/corporate/files/publications/strategies-action-plans/greening-sydney-strategy/greening-sydney-strategy.pdf?download=true.
[59] J. Polcyn, Y. Us, O. Lyulyov, T. Pimonenko, A. Kwilinski, Factors influencing the renewable energy consumption in selected european countries, Energies. 15 (2022) 1–27. https://doi.org/10.3390/en15010108.
[60] T. Kuronuma, H. Watanabe, T. Ishihara, D. Kou, K. Toushima, M. Ando, S. Shindo, CO2 Payoff of Extensive Green Roofs with Different Vegetation Species, Sustainability. 10 (2018) 2256. https://doi.org/10.3390/su10072256.
[61] C. Jansson, C. Faiola, A. Wingler, X.G. Zhu, A. Kravchenko, M.A. de Graaff, A.J. Ogden, P.P. Handakumbura, C. Werner, D.M. Beckles, Crops for Carbon Farming, Front. Plant Sci. 12 (2021) 1–12. https://doi.org/10.3389/fpls.2021.636709.
[62] P. Prosperi, M. Bloise, F.N. Tubiello, G. Conchedda, S. Rossi, L. Boschetti, M. Salvatore, M. Bernoux, New estimates of greenhouse gas emissions from biomass burning and peat fires using MODIS Collection 6 burned areas, Clim. Change. 161 (2020) 415–432. https://doi.org/10.1007/s10584-020-02654-0.
[63] M.R. Seyedabadi, U. Eicker, S. Karimi, Plant selection for green roofs and their impact on carbon sequestration and the building carbon footprint, Environ. Challenges. 4 (2021) 100119. https://doi.org/10.1016/j.envc.2021.100119.
[64] M. Foustalieraki, M.N. Assimakopoulos, M. Santamouris, H. Pangalou, Energy performance of a medium scale green roof system installed on a commercial building using numerical and experimental data recorded during the cold period of the year, Energy Build. 135 (2017) 33–38. https://doi.org/10.1016/j.enbuild.2016.10.056.

Supplementary Material

Supplementary Table 1. Specifications of the photovoltaic panels used on the BSGR and CSR.

Roof type	Bio-solar	Conventional
Panel model	SPR-MAX3-395	LG320N1K-V5
Manufacturer	Maxeon	LG
Solar Cells	104 Monocrystalline Gen 3	60 Monocrystalline / N-type
Dimensions (mm)	1046 x 1690 x 40 mm	1016 x 1686 x 40 mm
Nominal Power (pNom in W)	395	320
Power Tolerance (%)	+5/0	+3/0
Panel Efficiency (%)	22.3	18.7
Rated Voltage (V)	65.4	33.3
Rated Current (A)	6.04	9.62
Open-Circuit Voltage (V)	75.6	40.8
Short-Circuit Current (A)	6.57	10.19
Power Temp Coefficient (%)	−0.29 /°C	-0.38 /°C
Voltage Temp Coefficient (%)	−0.236 /°C	-0.28 /°C
Current Temp Coefficient (%)	0.058 /°C	0.03 /°C

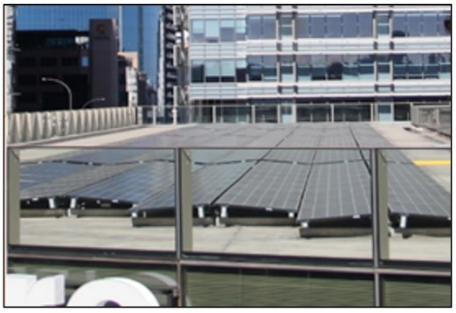

The CSR did not require any corrections as the BSGR was larger in size (kWp), more recently constructed, more efficient in converting solar energy, and possessed a better temperature coefficient.

Correct for system capacity:
Reduce output by ~15.54% to "size match" smaller CSR system.

Correct for age difference:
Reduce output by 1.2% to artificially "age" the newer system using the manufacturer specifications.

Correct for panel efficiency:
Reduce output by 3.1% to reduce the efficiency of the newer panels to match the "older technology" on the CSR.

Correct for differences in temperature coefficients:
Reduce output by -0.09%/1°C above 25°C to mimic the output loss experienced on the CSR.

Conduct analysis on the corrected "raw" data to determine differences in buildings without correcting for solar exposure

To account for variance in solar exposure between sites:
Conduct a multiple linear regression model to determine the performance of each roof based on a "standardised lighting scenario" using GHI, roof and season as predictors.

Supplementary Figure 1. Methodological infographic depicting the sequence of corrections applied to the BSGR to reduce the raw energy output to a state in which it is representative of the CSR energy output based on various factors and differences in system design.